Pion photoproduction in chiral bag models

M. Araki and A. N. Kamal
Theoretical Physics Institute and Department of Physics, University of Alberta, Edmonton, Alberta, Canada T6G 2J1
(Received 5 May 1983; revised manuscript received 23 September 1983)

Single-pion photoproduction is studied in two types of chiral bag models; the cloudy bag model with pseudoscalar coupling and a recently proposed model of Kälberman and Eisenberg. As the energy region studied encompasses the Δ mass, a finite-width Δ is used in our calculations. Detailed comparison with data is presented.

I. INTRODUCTION

Since the MIT bag model[1,2] was proposed almost ten years ago, it has been applied primarily in two directions: to generate the hadron spectra[3] and to study decay processes.[4] Of late a great deal of effort has gone into refining the model to accommodate chiral symmetry.[5–9]

Among the models that allow chiral symmetry, one of the most successful has been the cloudy bag model (CBM).[5] In this model the pionic degrees of freedom are introduced explicitly and the pions couple to the quarks only at the surface of the bag. The free pion field however exists inside the bag. The pion-quark coupling is pseudoscalar (PS). This model has met with success in describing several nucleon properties,[5] particularly the axial-vector coupling constant g_A and the neutron charge form factor. This model also describes the Δ resonance and pion-nucleon P-wave phase shifts in the $I=\frac{3}{2}$ state.

However, in order to describe the S-wave pion-nucleon scattering lengths, which are described well in current algebra,[10] one has to introduce a transformed quark field which introduces nonlinear pion-quark interaction.[8] More importantly, it also introduces a *volume* pion-quark interaction linear in the pion field of a pseudovector (PV) nature. It is this pseudovector pion-quark interaction which holds the key to the current-algebra result for S-wave pion-nucleon scattering lengths.

Recently, Kälberman and Eisenberg[9] (KE) have proposed a chiral bag model fashioned after Weinberg's σ-model formulation of chiral Lagrangian for the πN system.[11] The KE nonlinear chiral bag has pseudovector pion-quark coupling throughout the volume of the bag. In addition, the cubic and higher-order nonlinear terms in pion field in the KE bag model[9] differ from those of Thomas' bag model.[8]

The reader is reminded that single-pion production has been studied extensively in the past on the nucleon level.[12–16]

In this paper we have investigated pion photoproduction in the CBM[5] with PS surface coupling of pion with quarks and the KE model[9] with PV volume coupling of pion with quarks, well into the Δ region. In Sec. II, we define the interactions and the propagators. Pion photoproduction amplitudes and their multipole projections are calculated from the Born diagrams in Sec. III. In Sec. IV, we present numerical results for the low-order multipoles, single-pion production cross sections, and polarizations. A discussion of our results is also given in Sec. IV.

II. LAGRANGIANS AND PROPAGATORS

A. πqq interaction

In this section, we set up the basic tools of calculation. Throughout this paper we employ only the ground-state S-wave MIT bag wave function whose parameters are given by DeGrand, Jaffe, Johnson, and Kiskis.[2] The model, therefore, does not have any new parameters.

The original cloudy bag model[5] has a pseudoscalar coupling of the pion with the quarks only at the surface of the bag, of the form

$$\mathcal{L}^{\rm CBM}_{\pi qq}=-\frac{i}{2f}\sum_a \bar{q}_a(x)\vec{\tau}\cdot\vec{\pi}(x)\gamma_5 q_a\Delta_s\ , \tag{2.1}$$

where $\Delta_s=\delta(R-r)$. R is the bag radius.

It was subsequently shown[8] that by a redefinition of the quark field the linear PS pion-quark surface interaction could be transformed into a volume pseudovector term. We are interested in studying the consequences of the PS surface interaction (2.1) to single-pion photoproduction well into the Δ region. In the KE model[9] the pion-quark interaction is a pseudovector volume term of kind

$$\mathcal{L}^{\rm KE}_{\pi qq}=\frac{1}{2f}\sum_a \bar{q}_a(x)\gamma^\mu\gamma_5\vec{\tau}\cdot q_a(x)\partial_\mu\vec{\pi}(x)\theta_V\ , \tag{2.2}$$

where

$$\theta_V=\begin{cases}1, & r<R\ ,\\ 0, & r>R\ .\end{cases}$$

Notice that the derivative coupling of (2.2) induces a contact $\gamma\pi qq$ term by gauge invariance. Such a term is absent in the CBM description.

B. πNN interaction

The method of derivation of the πNN interaction Lagrangian starting from the πqq interaction of Eqs. (2.1) and (2.2) is given in Refs. 5 and 9. We give only the essential details.

The πNN interaction (as also $\pi N\Delta$, γNN, and $\gamma N\Delta$ interactions to follow) is defined in momentum space by

$$\mathscr{L}_{\pi NN}=\left\langle \pi_\alpha(\vec{q}),N(\vec{p}\,'\simeq 0)\,|\,\int_{\text{bag}} d^3x\,\mathscr{L}_{\pi qq}(x)\,|\,N(\vec{p}\simeq 0)\right\rangle . \tag{2.3}$$

The static MIT bag solution[1] with the lowest-frequency mode for massless quarks has the form

$$q_a(x)=\frac{N}{\sqrt{4\pi}}\begin{bmatrix} ij_0\left(\frac{\omega}{R}r\right) \\ -j_1\left(\frac{\omega}{R}r\right)\vec{\sigma}\cdot\hat{r}\end{bmatrix} u_m\chi_\alpha e^{-i\omega t}, \tag{2.4}$$

where

$$N^2=\frac{\omega}{2R^3(\omega-1)j_0^2(\omega)} . \tag{2.5}$$

In (2.4), u_m is the Pauli spin wave function and χ_α the isospin wave function of the quark. As shown in Ref. 5, one obtains $\mathscr{L}_{\pi NN}$ for the CBM as follows:

$$\mathscr{L}^{\text{CBM}}_{\pi NN}=-\frac{i}{2f}\left(\frac{\omega}{\omega-1}\right)\frac{j_1(qR)}{qR}\frac{5}{3}\left\langle N\,|\,\vec{\sigma}\cdot\vec{q}\tau_\alpha\,|\,N\right\rangle , \tag{2.6}$$

where $\vec{\sigma}$ and τ_α are the Pauli spin and isospin operators. $|\,N\rangle$ is the spin-isospin wave function of the nucleon.

Similarly, the KE bag model yields[9]

$$\mathscr{L}^{\text{KE}}_{\pi NN}=-\frac{i}{2f}\frac{5}{3}[R_0(j_0^2-\tfrac{1}{3}j_1^2)-\tfrac{4}{3}R_2(j_1^2)]\times\left\langle N\,|\,\vec{\sigma}\cdot\vec{q}\tau_\alpha\,|\,N\right\rangle , \tag{2.7}$$

where

$$R_l(f)\equiv N^2\int_0^R r^2dr\,j_l(qr)f\left(\frac{\omega}{R}r\right) . \tag{2.8}$$

The term $R_2(j_1^2)$ in Eq. (2.7) makes only a small contribution to the quantity in the square brackets.

A numerical test shows that the two interactions, Eqs. (2.6) and (2.7), are identical at $\vec{q}=0$ and even at $|\,\vec{q}\,|=300$ MeV/c they differ by less than 0.05%. This is perhaps not surprising in view of the work in Ref. 8. In Eqs. (2.6) and (2.7) one can identify (with M=nucleon mass)

$$g^{\text{CBM}}_{\pi NN}(\vec{q}^{\,2})/2M=\frac{5}{6f}\left(\frac{\omega}{\omega-1}\right)\frac{j_1(qR)}{qR} \tag{2.9}$$

and

$$g^{\text{KE}}_{\pi NN}(\vec{q}^{\,2})/2M=\frac{5}{6f}[R_0(j_0^2-\tfrac{1}{3}j_1^2)-\tfrac{4}{3}R_2(j_1^2)] . \tag{2.10}$$

At $\vec{q}^{\,2}=0$ both these couplings reduce to

$$g^{\text{CBM}}_{\pi NN}(0)\approx g^{\text{KE}}_{\pi NN}(0)\approx 0.8/f . \tag{2.11}$$

In Fig. 1 we have plotted the two strong form factors of Eqs. (2.9) and (2.10) for two values of R: $R=3.65$ and 5.0 GeV^{-1}. It is clear that numerically they are indistinguishable.

As the coupling constants are practically indistinguishable in the energy range we are interested in we shall, in practice, generate the NN vertex in the CBM[5] or in the KE model[9] by the use of the following PS or PV interaction Lagrangians with a form factor given in Eqs. (2.9) and (2.10):

$$\mathscr{L}^{\text{CBM}}_{\pi NN}=ig_{\pi NN}\bar{N}\gamma_5\vec{\tau}\cdot\vec{\pi}N , \tag{2.12}$$

$$\mathscr{L}^{\text{KE}}_{\pi NN}=\frac{2M}{m_\pi}g_{\pi NN}\bar{N}\gamma^\mu\gamma_5\vec{\tau}\cdot\partial_\mu\vec{\pi}N . \tag{2.13}$$

C. $\pi N\Delta$ interaction

In SU(6) symmetry one can write

$$2\sqrt{2}\left\langle N\,|\,\vec{\sigma}\cdot\vec{q}\vec{\tau}N\right\rangle=\tfrac{5}{3}\left\langle\Delta\,|\,\vec{S}\cdot\vec{q}\vec{T}\,|\,N\right\rangle , \tag{2.14}$$

where $\vec{S}$ and $\vec{T}$ are the transition spin and isospin operators defined in Refs. 17 and 18.

In analogy with Eqs. (2.6) and (2.7) the transition amplitude, in momentum space, is given by

$$\mathscr{L}_{\pi N\Delta}=-i\frac{g_{\pi N\Delta}(\vec{q}^{\,2})}{2M}\langle\Delta\,|\,\vec{S}\cdot\vec{q}\vec{T}\,|\,N\rangle , \tag{2.15}$$

where $|\,N\rangle$ and $|\,\Delta\rangle$ are spin-isospin wave functions for the nucleon and Δ. Also through SU(6) symmetry

$$g_{\pi N\Delta}(\vec{q}^{\,2})=\frac{6\sqrt{2}}{5}g_{\pi NN}(\vec{q}^{\,2}) . \tag{2.16}$$

D. γNN interaction

The photon-quark interaction Lagrangian density is given by

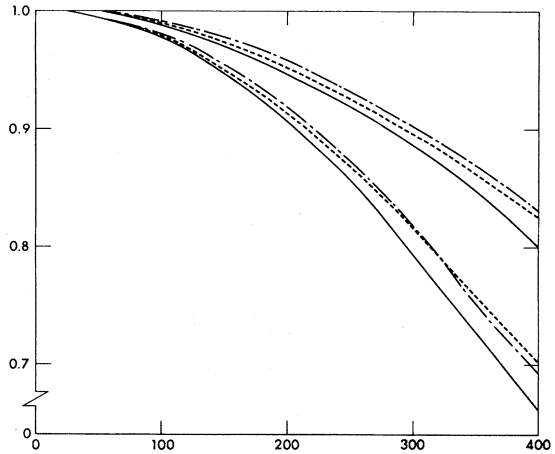

FIG. 1. Strong and electromagnetic form factors plotted vs k (in MeV). $g_{\pi NN}(k^2)/g_{\pi NN}(0)$ (solid curve); $G_E^0(k^2)/G_E^0(0)$ (dashed curve) and $G_M^0(k^2)/G_M^0(0)$ (dash-dot curve). Upper three curves are plotted for $R=3.65$ GeV^{-1} and the bottom three for $R=5.0$ GeV^{-1}.

$$\mathscr{L}_{\gamma qq} = -\sum_a eQ_a \bar{q}_a \gamma_\mu q_a A^\mu \,, \tag{2.17}$$

where $e>0$ and $Q_u=\frac{2}{3}$ and $Q_d=-\frac{1}{3}$.

Since nucleon form factors are used in our calculations we digress and reproduce the essential details. Define

$$\langle \gamma_\mu \rangle \equiv e\left\langle N \left| \int_{\text{bag}} d^3x\, \bar{q}_a(x)\gamma_\mu q_a(x) e^{i\vec{k}\cdot\vec{x}} \right| N \right\rangle . \tag{2.18}$$

Substituting (2.4) in (2.17), we obtain (note that these calculations have been done for ρNN vertex by Weber[19])

$$\langle \gamma_0 \rangle = eR_0(j_0{}^2+j_1{}^2)\delta_{mm'}\delta_{\alpha\beta} \,. \tag{2.19}$$

m,m' are the spin indices for the nucleon and α,β the isospin indices. Similarly,

$$\langle \vec{\gamma} \rangle = ieR_1(2j_0j_1)u^\dagger_{m'}(\vec{\sigma}\times\hat{k})u_m\delta_{\alpha\beta} \,. \tag{2.20}$$

Nucleon form factors $F_i(k^2)$ are defined via

$$\langle \gamma(k),N(p') \mid \mathscr{L}_{\gamma NN} \mid N(p) \rangle = \epsilon^\mu \bar{u}(p') \left[F_1(k^2)\gamma_\mu + iF_2(k^2)\frac{\sigma_{\mu\nu}k^\nu}{2M} \right] u(p) \,. \tag{2.21}$$

$F_i(k^2)$ are related[19] to the electric and magnetic form factors $G_E(k^2)$ and $G_M(k^2)$ through

$$F_1(\vec{k}^2) = \left[1+\frac{\vec{k}^2}{4M^2}\right]^{-1}\left[G_E(\vec{k}^2)+\frac{\vec{k}^2}{4M^2}G_M(\vec{k}^2)\right] \tag{2.22}$$

and

$$F_2(\vec{k}^2) = \left[1+\frac{\vec{k}^2}{4M^2}\right]^{-1}[G_M(\vec{k}^2)-G_E(\vec{k}^2)] \,. \tag{2.23}$$

Defining now the isospin dependence of the form factors through

$$G_E(\vec{k}^2) = \left[\frac{1+\tau_3}{2}\right]G_E^0(\vec{k}^2) \,, \tag{2.24}$$

$$G_M(\vec{k}^2) = \left[\tfrac{1}{6}+\tfrac{5}{6}\tau_3\right]G_M^0(\vec{k}^2) \,, \tag{2.25}$$

and

$$F_{1,2}(\vec{k}^2) = \tfrac{1}{2}[F_{1,2}^{(S)}(\vec{k}^2)+\tau_3 F_{1,2}^{(V)}(\vec{k}^2)] \,, \tag{2.26}$$

we find

$$G_E^0(\vec{k}^2) = eR_0(j_0{}^2+j_1{}^2) = e\left[1-\frac{\vec{k}^2}{6}\langle r^2\rangle+\frac{\vec{k}^4}{120}\langle r^4\rangle-\cdots\right], \tag{2.27}$$

where

$$\langle r^n \rangle = N^2\int_0^R r^{n+2}dr\left[j_0{}^2\left[\frac{\omega}{R}r\right]+j_1{}^2\left[\frac{\omega}{R}r\right]\right] \tag{2.28}$$

and

$$G_M^0(\vec{k}^2) = \frac{2Me}{|\vec{k}|}R_1(2j_0j_1) = 2Me\left[\tfrac{2}{3}I_1(R)-\tfrac{1}{15}\vec{k}^2 I_2(R)+\cdots\right], \tag{2.29}$$

where

$$I_n(R) = N^2\int_0^R r^{2n+1}dr\, j_0\left[\frac{\omega}{R}r\right]j_1\left[\frac{\omega}{R}r\right] . \tag{2.30}$$

With $\omega=2.04$, we get

$$\langle r^2\rangle = 0.53R^2, \quad \langle r^4\rangle = 0.384R^4 \tag{2.31}$$

and

$$\mu_p = \tfrac{2}{3}I_1(R) = 0.203R, \quad I_2(R) = 0.244R^3 \,, \tag{2.32}$$

where μ_p is the proton magnetic moment.

In Fig. 1 we have plotted $G_E^0(\vec{k}^2)$ and $G_M^0(\vec{k}^2)$ as functions of $\vec{k}^2$.

E. $\gamma N\Delta$ interaction

Using the photon-quark interaction Lagrangian of Eq. (2.17), one derives the $\gamma N\Delta$ interaction, in momentum space, as

$$\mathscr{L}_{\gamma N\Delta} = -i\frac{\sqrt{2}}{M}G_M^0(\vec{k}^2)\langle \Delta \mid (\vec{S}\times\vec{k})\cdot\vec{\epsilon}T_3 \mid N\rangle \,, \tag{2.33}$$

where $G_M^0(k^2)$ is defined in Eqs. (2.22)—(2.29).

A phenomenological Lagrangian of a gauge-invariant form which simulates (2.33) is

$$\mathscr{L}_{\gamma N\Delta} = -ieC\psi^{\dagger\mu}_\Delta T_3\gamma^\nu\gamma_5\psi_N F_{\mu\nu} + \text{H.c.} \tag{2.34}$$

Reducing (2.34) nonrelativistically and keeping only the dominant M_{1+} term[20] one obtains

$$\mathscr{L}_{\gamma N\Delta} = -ie\frac{C}{4}\frac{(M+M_\Delta)^2}{MM_\Delta}\langle \Delta \mid (\vec{S}\times\vec{k})\cdot\vec{\epsilon}T_3 \mid N\rangle \,. \tag{2.35}$$

Comparing (2.33) with (2.35) one obtains

$$C = \frac{4\sqrt{2}M_\Delta}{(M+M_\Delta)^2}\frac{G_M^0(\vec{k}^2)}{e} \,. \tag{2.36}$$

Using

$$G_M^0(0) = 1.9e \,, \tag{2.37}$$

we get

$$C = \begin{cases} 0.28/m_\pi, & \text{for } R=3.65 \text{ GeV}^{-1} \,, \\ 0.39/m_\pi, & \text{for } R=5.0 \text{ GeV}^{-1} \,. \end{cases} \tag{2.38}$$

This is to be compared with $c=0.37/m_\pi$ given by Gourdin and Salin.[21] We shall use the Lagrangian in Eq. (2.34) with C given by (2.36).

F. Seagull term

The minimal replacement, $\partial_\mu\to\partial_\mu-ieA_\mu$, in Eq. (2.2) leads to a seagull term

$$\mathscr{L}_{\gamma\pi qq} = \frac{e}{2f}\epsilon_{bc3}\sum_a \bar{q}_a \not{\pi}\gamma_5\tau_b q_a \pi_c \theta_V \,. \tag{2.39}$$

In the Coulomb gauge, $\epsilon_0=0$, one obtains the following $\gamma\pi NN$ contact term in momentum space;

$$\mathscr{L}_{\gamma\pi NN}=\frac{ie}{2f}\frac{5}{3}\{[R_0(j_0{}^2-\tfrac{1}{3}j_1{}^2)+\tfrac{2}{3}R_2(j_1{}^2)](\vec{\epsilon}\cdot\vec{\sigma})-2R_2(j_1{}^2)(\vec{\epsilon}\cdot\hat{q})(\vec{\sigma}\cdot\hat{q})\}\tfrac{1}{2}[\tau_c,\tau_3] \tag{2.40a}$$

$$\approx ie\frac{g_{\pi NN}(q^2)}{2M}[\vec{\sigma}\cdot\vec{\epsilon}-0.546j_2(qR)(\vec{\epsilon}\cdot\hat{q})(\vec{\sigma}\cdot\hat{q})]\tfrac{1}{2}[\tau_c,\tau_3]\ . \tag{2.40b}$$

Equation (2.40b) is a convenient numerical approximation to (2.40a). $g_{\pi NN}(q^2)$ can be read off Eq. (2.11) in the KE model

$$g^{\rm KE}_{\pi NN}(q^2)/2M=\frac{5}{3}\frac{1}{2f}[R_0(j_0{}^2-\tfrac{1}{3}j_1{}^2)-\tfrac{4}{3}R_2(j_1{}^2)]$$
$$\approx\frac{5}{3}\frac{1}{2f}R_0(j_0{}^2-\tfrac{1}{3}j_1{}^2)\ . \tag{2.41}$$

The last line follows from the fact that $R_2(j_1{}^2)$ makes only a small contribution. Note that if one were to use the PV coupling, Eq. (2.13), on the nucleon level and then generate the seagull term by the minimal replacement one would have obtained only the $\vec{\sigma}\cdot\vec{\epsilon}$ part of Eq. (2.40b). The tensor term generated by working with PV coupling on the quark level in Eq. (2.40b) is, however, very small in comparison.

In practice we shall work with the PV πNN coupling of Eq. (2.13) and introduce by hand the extra tensor contribution contained in Eq. (2.40b) which would otherwise not be generated.

G. Propagators

DeTar[7] has written down the nonrelativistic forms of the nucleon and the Δ propagators. For applications well into the Δ region we use the relativistic forms of the propagators:

$$\text{Nucleon: }\frac{i(\not{p}+M)}{p^2-M^2+i\epsilon}\ , \tag{2.42}$$

$$\Delta\text{: }\frac{P_{\mu\nu}}{p^2-M_\Delta{}^2+iM_\Delta\Gamma(\vec{\rm p}^{\,2})}\ , \tag{2.43}$$

where

$$P_{\mu\nu}=-\left[g_{\mu\nu}-\tfrac{1}{3}\gamma_\mu\gamma_\nu-\frac{1}{3M}(\gamma_\mu p_\nu-p_\mu\gamma_\nu)-\frac{2p_\mu p_\nu}{3M^2}\right](\not{p}+M)\ . \tag{2.44}$$

The width $\Gamma(\vec{\rm p}^{\,2})$ is given by

$$\Gamma(\vec{\rm p}^{\,2})=\frac{[g_{\pi N\Delta}(\vec{\rm p}^{\,2}=0)]^2}{18\pi M_\Delta}\left[\frac{|\vec{\rm p}|^3}{\omega_p+E_p}\right]h^2(\vec{\rm p}^{\,2})\ , \tag{2.45}$$

where

$\vec{\rm p}=$ center-of-mass momentum ,

$h(\vec{\rm p}^{\,2})=g_{\pi N\Delta}(\vec{\rm p}^{\,2})/g_{\pi N\Delta}(0)$,

$\omega_p=(\vec{\rm p}^{\,2}+m_\pi{}^2)^{1/2}$, $E_p=(\vec{\rm p}^{\,2}+M^2)^{1/2}$.

In SU(6) symmetry, because of the closeness of $g_{\pi NN}(\vec{\rm p}^{\,2})$ in the CBM and the KE model, the Δ width has the same value in both these models. We digress briefly to investigate the behavior of the P_{33} phase shift in πN scattering as predicted by the two models.

The method of analysis is given in Refs. 5, 22, and 23. The idea is to start with a "bare" Δ pole in the direct channel as the driving term in the Blankenbecler-Sugar[24] equation. A mass shift and the width are then generated by πN bubbles. To wit, one uses the Blankenbecler-Sugar equation[24]

$$T(\vec{\rm p},\vec{\rm q};s)=V(\vec{\rm p},\vec{\rm q};s)+\int\frac{d^3\vec{\rm k}}{(2\pi)^3}\frac{1}{2\omega_kE_k}V(\vec{\rm p},\vec{\rm k};s)\times\frac{(\omega_k+E_k)}{(\omega_k+E_k)^2-s-i\epsilon}T(\vec{\rm k},\vec{\rm q};s)\ , \tag{2.46}$$

where

$$V(\vec{\rm p},\vec{\rm q};s)=\frac{\mathscr{U}^\dagger(\vec{\rm p})\mathscr{U}(\vec{\rm q})}{s-M_\Delta{}^2} \tag{2.47}$$

with

$$\mathscr{U}(\vec{\rm q})=g_{\pi N\Delta}(\vec{\rm q}^{\,2})\vec{\rm S}\cdot\vec{\rm q}\,Th(\vec{\rm q}^{\,2})\ . \tag{2.48}$$

The solution of the Blankenbecler-Sugar equation is then written as

$$T(\vec{\rm p},\vec{\rm q};s)=\frac{\mathscr{U}^\dagger(\vec{\rm p})\mathscr{U}(\vec{\rm q})}{D(s)}\ , \tag{2.49}$$

where

$$D(s)=s-M_\Delta{}^2+\frac{1}{9\pi^2}\int_0^\infty dk\frac{k^4[g_{\pi N\Delta}(\vec{\rm k}^{\,2})]^2}{(\omega_k+E_k)^2-s-i\epsilon}\times\frac{(\omega_k+E_k)}{\omega_kE_k}\ . \tag{2.50}$$

One then derives the result written in (2.45) from the imaginary part of $D(s)$ and the scattering phase shift from

$$p^3\cot\delta(p)=\frac{18\pi s^{1/2}}{[g_{\pi N\Delta}(\vec{\rm p})]^2}\left\{M_\Delta{}^2-s-\frac{1}{9\pi^2}{\rm P}\int_0^\infty dk\frac{k^4[g_{\pi N\Delta}(\vec{\rm k}^{\,2})]^2}{(\omega_k+E_k)^2-s}\frac{(\omega_k+E_k)}{\omega_kE_k}\right\}\ . \tag{2.51}$$

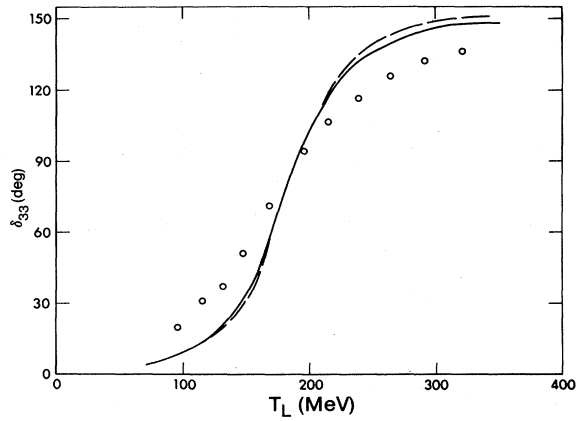

FIG. 2. P_{33} phase shift vs pion laboratory kinetic energy. Data from Ref. 26. Solid curve $R=3.65$ GeV^{-1}. Dashed curve $R=5.0$ GeV^{-1}.

In Fig. 2 we have plotted $\delta(p)$ as a function of momentum for bag radii, $R=3.65$ GeV^{-1} and 5.0 GeV^{-1}. The results for the CBM and KE model are indistinguishable as anticipated. A width of 60 MeV is obtained, consistent with one of 50 MeV obtained in a chiral bag.[25]

III. PION PHOTOPRODUCTION AMPLITUDES

We follow the notation of Ref. 13 with metric $g^{00}=1$, $g^{ii}=-1$. For completeness we reproduce the essential details but relegate standard definitions to the Appendix.

The transition amplitude for

$$\gamma(k)+N(p_1)\rightarrow\pi_\alpha(q)+N(p_2)$$

is written as

$$T_{fi}=\bar{u}_f(p_2)\sum_{j=1}^{4}A_j(s,t)M_j^\mu\epsilon_\mu u(p_1)\ . \tag{3.1}$$

The gauge-invariant spin matrices[13,14] M_j^μ are written down in the Appendix. The Mandelstam variables (s,t,u) and the isospin projections of $A_j(s,t)$ are also defined in the Appendix.

In evaluating the Born amplitude we have used the PS and PV interactions of Eqs. (2.12) and (2.13) with the strong form factors given by Eqs. (2.10) and (2.11). In practice there is no noticeable difference between the CMB and the KE πNN vertices. The latter, however, does produce a seagull term of type $\vec{\sigma}\cdot\vec{\epsilon}$ of Eq. (2.40b). The additional tensor term in Eq. (2.40b) is fed in by hand.

For the γNN vertex the electromagnetic form factors discussed in Sec. II are used.

The Born amplitude with nucleon poles and the contact term [without as yet the tensor term of Eq. (2.40b)] can be written in the following form:[13]

$$\tilde{A}^{\rm KE}=\tilde{A}^{\rm CBM}+\tilde{\Gamma}^{\rm PV} \tag{3.2}$$

with

$$\tilde{A}^{\rm CBM}=\left[\frac{1}{s-M^2}+[\tilde{\xi}]\frac{1}{u-M^2}\right]\tilde{\Gamma}(t)\ , \tag{3.3}$$

where $\tilde{A}$ is a vector with components $A_1,\ldots,A_4$, $[\tilde{\xi}]$ is a diagonal matrix with $[\xi]=\xi\,\mathrm{diag}(1,1,-1,1)$, and ξ is a parameter defined by $\xi^{(+,0,-)}=(1,1,-1)$. The residue vector $\tilde{\Gamma}(t)$ is defined by

$$\Gamma_1^{(\pm,0)}=\tfrac{1}{2}g_{\pi NN}(\vec{q}^{\,2})F_1^{(V,S)}(\vec{k}^{\,2})\ , \tag{3.4}$$

$$\Gamma_2^{(\pm,0)}=\frac{g_{\pi NN}(\vec{q}^{\,2})}{m_\pi^{\,2}-t}F_1^{(V,S)}(\vec{k}^{\,2})\ , \tag{3.5}$$

$$\Gamma_3^{(\pm,0)}=\Gamma_4^{(\pm,0)}=-\tfrac{1}{2}g_{\pi NN}(\vec{q}^{\,2})F_1^{(V,S)}(\vec{k}^{\,2})\ , \tag{3.6}$$

and

$$\Gamma_1^{\rm PV}=\frac{e}{2}(1+\xi)\frac{g_{\pi NN}(\vec{q}^{\,2})}{2M}F_2^{(V,S)}(\vec{k}^{\,2}) \tag{3.7}$$

$$\Gamma_2^{\rm PV}=\Gamma_3^{\rm PV}=\Gamma_4^{\rm PV}=0\ . \tag{3.8}$$

The strong and electromagnetic form factors are defined in Sec. II.

The Δ-pole terms are similarly obtained as follows:[13]

$$\tilde{A}_\Delta(s,t)=\left[\frac{1}{s-M_\Delta^{\,2}+iM_\Delta\Gamma(s)}+[\tilde{\xi}]\frac{1}{u-M_\Delta^{\,2}}\right]\tilde{\Delta}(t)+\tilde{A}_{np}(s,t)\ , \tag{3.9}$$

where

$$\tilde{\Delta}(t)=\eta\begin{bmatrix}\frac{1}{8}\left[4t+\frac{4M}{3M_\Delta}(M_\Delta^{\,2}-M^2+2m_\pi^{\,2})+\frac{4M^2}{3M_\Delta^{\,2}}(M_\Delta^{\,2}-M^2+m_\pi^{\,2})\right]\\ -1\\ \frac{1}{8}\left[-(2M+4M_\Delta)+\frac{4M^2}{3M_\Delta}+\frac{2M}{3M_\Delta^{\,2}}(M_\Delta^{\,2}-2M^2+2m_\pi^{\,2})\right]\\ \frac{1}{8}\left[6M+4M_\Delta+\frac{4M^2}{3M_\Delta}+\frac{2M}{3M_\Delta^{\,2}}(M_\Delta^{\,2}-2M^2+2m_\pi^{\,2})\right]\end{bmatrix} \tag{3.10}$$

with

$$\eta^{(+,0,-)}=(-2,0,1)\frac{e}{3}g_{\pi N\Delta}(q^2)\frac{C(k^2)}{2M} . \tag{3.11}$$

The nonpole part is

$$\tilde{A}_{np}^{(+)}(s,t)=-\eta^{(+)}\begin{pmatrix}\frac{1}{6M_\Delta{}^2}[t-m_\pi{}^2-2M(M+M_\Delta)]\\0\\0\\\frac{1}{3M_\Delta{}^2}(M_\Delta-M)\end{pmatrix}, \tag{3.12}$$

$$\tilde{A}_{np}^{(0)}=0 , \tag{3.13}$$

$$\tilde{A}_{np}^{(-)}=-\eta^{(-)}\begin{pmatrix}\frac{1}{6M_\Delta{}^2}(u-s)\\0\\\frac{1}{3M_\Delta{}^2}(M_\Delta-M)\\0\end{pmatrix} . \tag{3.14}$$

The transition strong and electromagnetic form factors are given in Sec. II. The expressions in Eqs. (3.10)—(3.14) correspond to the case $\alpha=\beta=-1$ of Olsson and Osypowski.[13]

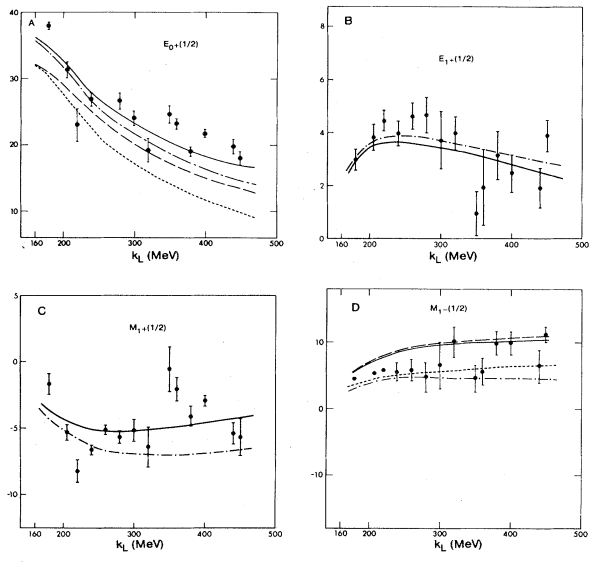

FIG. 3. Real parts of electric and magnetic multipoles for $I=\frac{1}{2}$ in units of $10^{-3}/m_\pi$. Solid curve: KE model. Dashed curve: CBM. Dash-dot curve: PV (no-bag). Dotted curve: PS (no-bag). Where the two bag-model predictions and the two no-bag predictions cannot be distinguished, a solid curve is used for bag-model predictions and dash-dot curve for no-bag predictions. Experimental points from Ref. 27. Bag radius: $R=3.65$ GeV^{-1}.

In order to extract the multipoles, one defines a scattering amplitude, in the center of mass, through

$$f_{fi}=\frac{M}{4\pi W}T_{fi} \tag{3.15}$$

and expands[13,14] f_{fi} in terms of Pauli spin matrices as

$$f_{fi}=\chi_f^+\mathcal{F}\chi_i \tag{3.16}$$

with

$$\mathcal{F}=i\vec{\sigma}\cdot\vec{\epsilon}\mathcal{F}_1+(\vec{\sigma}\cdot\hat{q})\vec{\sigma}\cdot(\hat{k}\times\vec{\epsilon})\mathcal{F}_2 +i(\vec{\sigma}\cdot\hat{k})(\vec{\epsilon}\cdot\hat{q})\mathcal{F}_3+i(\vec{\sigma}\cdot\hat{q})(\vec{\epsilon}\cdot\hat{q})\mathcal{F}_4 . \tag{3.17}$$

The relations between $\mathcal{F}_i$ and A_j are written down in the Appendix. Notice that the tensor term of Eq. (2.40b) makes its appearance in $\mathcal{F}_4$.

The multipoles are then projected by the usual prescription given in Refs. 13 and 14. The multipoles in a specific isospin in the final state are obtained from

$$\begin{aligned}M_l(\tfrac{1}{2})&=M_l^{(+)}+2M_l^{(-)} ,\\ M_l(\tfrac{3}{2})&=M_l^{(+)}-M_l^{(-)} .\end{aligned} \tag{3.18}$$

IV. RESULTS AND DISCUSSION

We have calculated the low-order multipoles ($l\leq 2$), total cross section, angular distributions, and polarizations in the CBM[5] and the KE[9] model. In the calculations, based on nucleon and Δ-pole diagrams, together with the seagull term for the KE model, strong and electromagnetic form factors as predicted by the bag models are used.

The real parts of the electric and magnetic multipoles for $I=\frac{1}{2}$ final state are plotted in Figs. 3(A)—3(D) for the CBM and the KE model for bag radius $R=3.65$ GeV^{-1}.

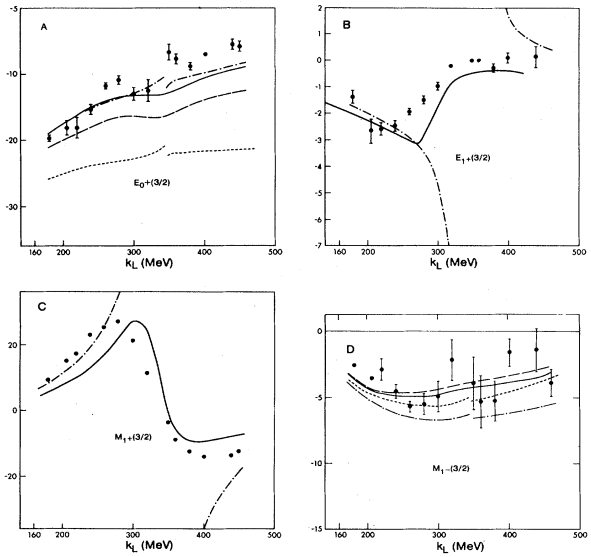

FIG. 4. Real parts of electric and magnetic multipoles for $I=\frac{3}{2}$ in units of $10^{-3}/m_\pi$. See caption to Fig. 3 for details.

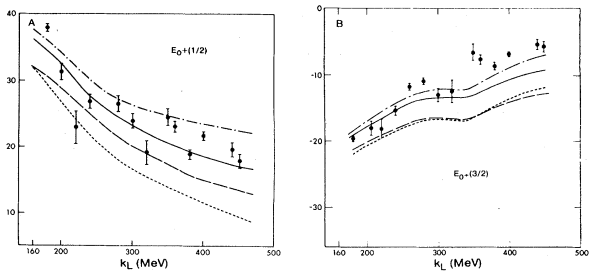

FIG. 5. R dependence of $E_{0+}(\frac{1}{2})$ and $E_{0+}(\frac{3}{2})$. 5(A) Real part of $E_{0+}(\frac{1}{2})$. (B) Real part of $E_{0+}(\frac{3}{2})$. KE model: solid curve: $R=3.65$ GeV^{-1}; Dash-dot curve: $R=5.0$ GeV^{-1}. CBM: Dashed curve: $R=3.65$ GeV^{-1}; Dotted curve: $R=5.0$ GeV^{-1}.

For comparison we have also plotted the multipoles as calculated from the Olsson-Osypowski[13] formalism with PV coupling with their parameters $\alpha=\beta=-1$. The two bag models give identical results for all multipoles except the dipoles $E_{0+}(\frac{1}{2})$ and $M_{1-}(\frac{1}{2})$. It is known[16] that on the nucleon level the PS and PV theories also agree on all multipoles except the electric and magnetic dipoles mentioned above.

In Figs. 4(A)—4(D) we have plotted the electric and magnetic multipoles for the $I=\frac{3}{2}$ final state with the bag radius $R=3.65$ GeV^{-1}. For comparison the Olsson-Osypowski[13] predictions, with zero width Δ, are also plotted. The discontinuity at the Δ mass is a result of the zero-width approximation. Our calculation uses a finite but a narrow (60 MeV) Δ width. With a larger Δ width the structure in the $I=\frac{3}{2}$ multipoles at the Δ mass would be considerably smoothed out. Again the CBM and the KE model make identical predictions for all multipoles except the dipoles $E_{0+}(\frac{3}{2})$ and $M_{1-}(\frac{3}{2})$. In Fig. 5 we have plotted the R dependence of our results for $E_{0+}(\frac{1}{2})$ and $E_{0+}(\frac{3}{2})$.

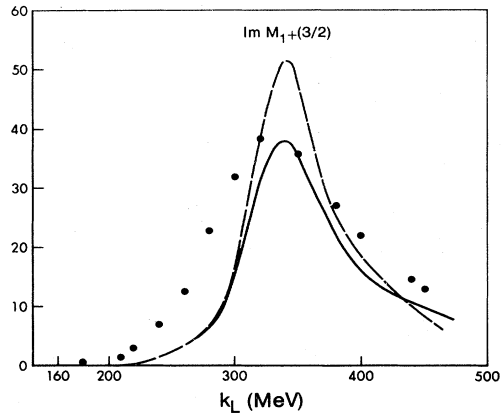

FIG. 6. Imaginary part of M_{1+} for $I=\frac{3}{2}$ in units of $10^{-3}/m_\pi$ in the two bag models. The results in the two models are indistinguishable. Experimental points from Ref. 27. Bag radius: $R=3.65$ GeV^{-1}.

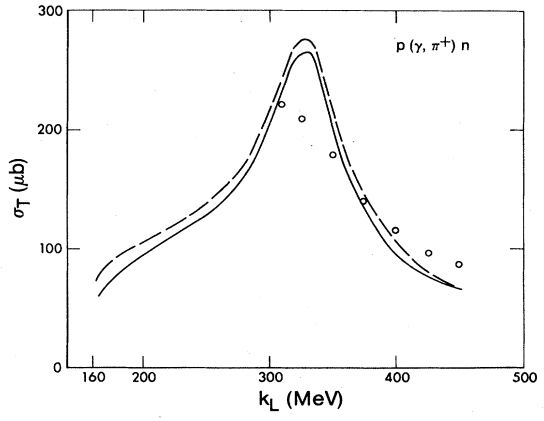

FIG. 7. Total cross sections for $p(\gamma,\pi^+)n$. Experimental points from Ref. 28. Results in the two bag models are indistinguishable. Solid curve: $R=3.65$ GeV^{-1}. Dashed curve: $R=5.0$ GeV^{-1}.

Im$M_{1+}(\frac{3}{2})$ is plotted in Fig. 6 with bag radii $R=3.65$ GeV^{-1} and 5.0 GeV^{-1}. The peak appears to be a better fit by the lower radius. The theoretical peak is much narrower than the data. The same feature is exhibited by the total cross section for $p(\gamma,\pi^+)n$ plotted in Fig. 7. An explanation of our results and comparison with the work of the CBM[5] follows.

In our calculation the driving term in the Blankenbecler-Sugar equation for the P_{33} πN amplitude is the bare-Δ direct-channel pole. We neglect the P_{33} projection of the cross nucleon term which would produce the "Chew-Low" part of the driving term used in Ref. 5. Thus in Ref. 5 the P_{33} πN amplitude has the Δ pole as we have and, in addition, a background term which provides the extra width of the P_{33} amplitude at Δ resonance, a part which is missing from our work. The Δ width we obtain (60 MeV) is consistent with the width resulting from Δ pole in Ref. 5.

The angular distributions for $p(\gamma,\pi^0)p$ at photon energies 180 and 360 MeV are plotted in Fig. 8 and that for

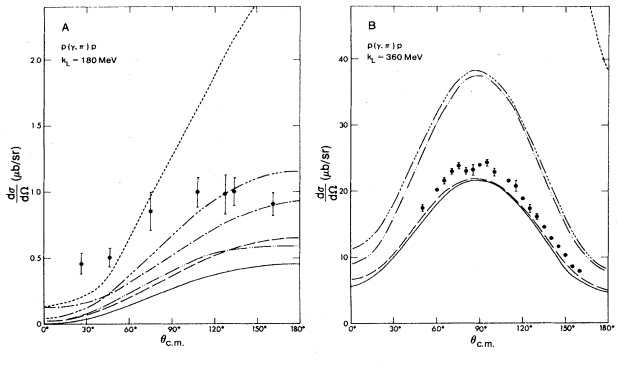

FIG. 8. Angular distribution for $p(\gamma,\pi^0)p$ at 180 (a), 360 MeV (b); Experimental points from Refs. 29 and 30. ——: KE with $R=3.65$ GeV^{-1}. —.—: KE with $R=5.0$ GeV^{-1}. — — —: CBM with $R=3.65$ GeV^{-1}. —·—·—: CBM with $R=5.0$ GeV^{-1}. —·—·—·—: PV (no bag). — — —: PS (no bag).

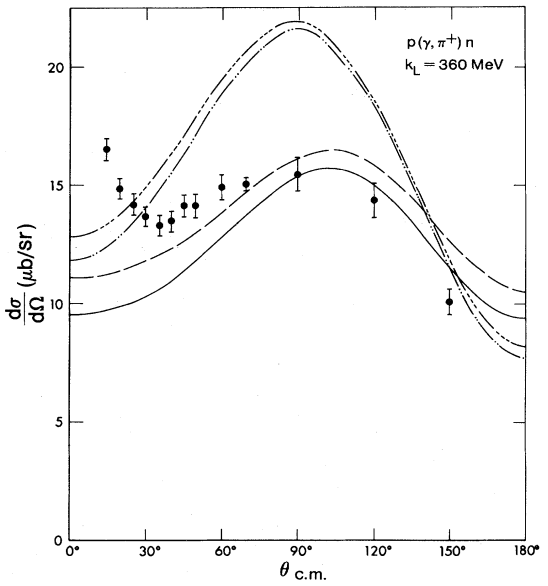

FIG. 9. Angular distribution for $p(\gamma,\pi^+)n$ at 360 MeV. See caption to Fig. 8 for details. Experimental points from Ref. 31.

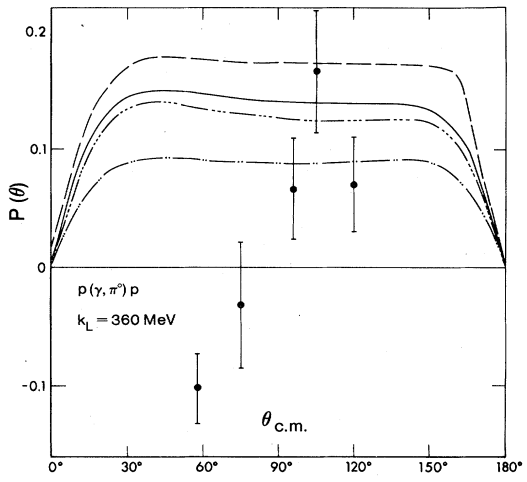

FIG. 10. Polarization for $p(\gamma,\pi^0)p$ at 360 MeV. Experimental points from Ref. 32. See caption to Fig. 8 for details.

$p(\gamma,\pi^+)n$ at 360 MeV in Fig. 9. Polarization for $p(\gamma,\pi^0)p$ at 360 MeV is plotted in Fig. 10. For all these plots we use two bag radii $R=3.65$ and 5.0 GeV^{-1}.

We wish to note here that all the results obtained in the present analysis with the KE model would be the same as the PV version of the CBM[8] since both models are equivalent up to terms quadratic in pion field. In this paper by the CBM we mean the PS version of the CBM.[5] The general conclusion we draw is that the KE model, based on a PV coupling, with a smaller bag radius of 3.65 GeV^{-1}, fits data reasonably well. This is not surprising in view of the fact that, on the nucleon level, the PV theory with nucleon and pion poles and the seagull terms leads to the low-energy theorems derived from PCAC (partial conservation of axial-vector current) and current algebra for photoproduction of single pions, charged or neutral.[12,16,33–36] Both the KE model and the CBM Lagrangian satisfy PCAC in contrast to the PS theory on the nucleon level, but this does not imply that the Born terms in the two models would be the same. The reason that the CBM (or the PS coupling on nucleon level) does not fare as well at low energies in our calculations has more to do with the difficulty of doing a complete calculation than with an inherent problem with the theory. It is known[36] that the PS theory on the nucleon level with nucleon and pion poles alone gives quite a good fit to the threshold charged-pion photoproduction amplitude E_{0+} but rather a poor fit to neutral-pion photoproduction. Inclusion of the dispersion contribution, particularly the s- and u-channel Δ resonances, improves[36] the situation. One expects that the t-channel contribution (ω exchange, for example) would also play a role at threshold[15] for π^0 photoproduction. In contrast, the inclusion of the Δ resonances makes very little difference to the charged-pion photoproduction[36] at threshold.

We end this section with a discussion of the role of the seagull term and its equivalent in the PS theory.

In the PS theory the amplitude generated by the two nucleon-pole terms (s- and u-channel) and the pion-pole term satisfies gauge invariance. In the PV theory the seagull term is required by gauge invariance. If one were to work in the Coulomb gauge, $\epsilon_0=0$, and split the nucleon-pole contribution into positive energy nucleon intermediate state and the Z graphs (nucleon-antinucleon pair in intermediate state) one can show that at threshold only the Z graphs contribute.

The seagull terms contribute only to charged-pion photoproduction. Also the Z-graph contribution in the PV theory is of order m_π/M at pion production threshold. PS theory, on the other hand, yields a Z-graph contribution of order unity. Since for neutral-pion photoproduction Z graphs are the only contributors in *both* PS and PV theories, the latter theory leads to a smaller amplitude in agreement[16] with experiments.

For charged-pion photoproduction the seagull term compensates for the small contribution of the Z graphs in the PV theory. In this sense the seagull term simulates the effect of Z graphs in the PS theory. The net effect is that the PS and the PV theories lead to almost identical amplitudes for charged-pion photoproduction.

Subtle differences remain between the PS and PV theories on the Born level. The PV theory leads to correct dipole amplitudes E_{0+} and M_{1-} in both $I=\frac{1}{2}$ and $\frac{3}{2}$ final states in contradiction to the PS theory. Both theories on the Born level, however, produce identical higher multipoles.[16]

ACKNOWLEDGMENTS

This research was partly supported by a grant from the Natural Sciences and Engineering Research Council of Canada to A. N. K. We thank Dr. Y. Nakano for discussions and a check on some of the analytical calculations.

APPENDIX

The gauge-invariant spin matrices M_j^μ are[13,14]

$$\begin{aligned} M_1^\mu &= i\gamma_5\gamma^\mu \not{k} , \\ M_2^\mu &= 2i\gamma_5[P^\mu(q\cdot k)-(P\cdot k)q^\mu] , \\ M_3^\mu &= \gamma_5[\gamma^\mu(q\cdot k)-\not{k}q^\mu] , \\ M_4^\mu &= 2\gamma_5[\gamma^\mu(P\cdot k)-\not{k}P^\mu - iM\gamma^\mu\not{k}] , \end{aligned} \tag{A1}$$

where $P=\frac{1}{2}(p_1+p_2)$.

The Mandelstam variables are

$$s=(k+p_1)^2, \quad t=(q-k)^2, \quad u=(k-p_2)^2 . \tag{A2}$$

The isospin structure of the amplitude is given in terms of the three projection operators

$$A_j = A_j^{(+)}\delta_{\alpha 3} + A_j^{(-)}\tfrac{1}{2}[\tau_\alpha,\tau_3] + A_j^{(0)}\tau_3 . \tag{A3}$$

The relations between $\mathcal{F}_j$ and A_j are as follows:

$$\begin{aligned} \mathcal{F}_1 &= F\left[A_1+(W-M)A_4-\frac{(t-m_\pi{}^2)}{2(W-M)}(A_3-A_4)\right] , \\ \mathcal{F}_2 &= qF\left[-A_1+(W+M)A_4-\frac{(t-m_\pi{}^2)}{2(W+M)}(A_3-A_4)\right] , \\ \mathcal{F}_3 &= qF[(W-M)A_2+(A_3-A_4)] , \\ \mathcal{F}_4 &= q^2F\left[-(W+M)A_2+(A_3-A_4) + (\xi-1)\frac{5ef_{\pi NN}}{3m_\pi g_A}\frac{R_2(j_1{}^2)}{(W-M)q^2}\right] , \end{aligned} \tag{A4}$$

where

$$\begin{aligned} F &= \left[\frac{W-M}{8\pi W}\right](D_1D_2)^{1/2} , \\ D_1 &= M+(M^2+\vec{k}^{\,2})^{1/2} , \\ D_2 &= M+(M^2+\vec{q}^{\,2})^{1/2} , \\ W &= \text{total c.m. energy} . \end{aligned} \tag{A5}$$

[1] A. Chodos, R. L. Jaffe, K. Johnson, C. B. Thorn, and V. F. Weisskopf, Phys. Rev. D 9, 3471 (1974); K. Johnson, Acta Phys. Pol. B6, 865 (1975).

[2] T. A. DeGrand, R. L. Jaffe, K. Johnson, and J. Kiskis, Phys. Rev. D 12, 2060 (1975).

[3] R. L. Jaffe and J. Kiskis, Phys. Rev. D 13, 1355 (1976); R. L. Jaffe, *ibid.* 15, 267 (1976); A. J. G. Hey, in *Topics in Quantum Field Theory and Gauge Theories,* proceedings of the VIIIth International Seminar on Theoretical Physics, Salamanca, Spain, 1977 (Lecture Notes in Physics No. 77), edited by J. A. de Azcarraga (Springer, Berlin, 1978), p. 155.

[4] See, for example, Lo Chong-Hua, Phys. Rev. D 26, 199 (1982); J. F. Donoghue and B. R. Holstein, *ibid.* 25, 206 (1982).

[5] S. Théberge, A. W. Thomas, and G. A. Miller, Phys. Rev. D 22, 2838 (1980); 23, 2106(E) (1981); Can. J. Phys. 60, 59 (1982); A. W. Thomas, CERN Report No. TH. 3368-CERN (unpublished); TRIUMF Report No. TRI-PP-82-29, 1982 (unpublished).

[6] V. M. Vento, M. Rho, E. M. Nyman, and G. E. Brown, Nucl. Phys. A345, 413 (1980).

[7] C. E. DeTar, Phys. Rev. D 24, 752 (1981); 24, 762 (1981).

[8] A. W. Thomas, J. Phys. G 7, L283 (1981).

[9] G. Kälberman and J. M. Eisenberg, Phys. Rev. D 28, 66 (1983); 28, 71 (1983).

[10] S. Weinberg, Phys. Rev. Lett. 17, 616 (1966).

[11] S. Weinberg, Phys. Rev. Lett. 18, 188 (1967).

[12] N. Dombey and B. J. Read, Nucl. Phys. B60, 65 (1973).

[13] M. G. Olsson and E. T. Osypowski, Nucl. Phys. B87, 399 (1975); A. Donnachie, in *High Energy Physics,* edited by E. H. S. Burhop (Academic, New York, 1972), Vol. 6, p. 1.

[14] G. F. Chew, M. L. Goldberger, F. E. Low and Y. Nambu, Phys. Rev. 106, 1345 (1967).

[15] F. A. Berends, A. Donnachie, and D. L. Weaver, Nucl. Phys. B4, 1 (1967); B4, 54 (1967); B4, 103 (1967).

[16] J. M. Laget, Phys. Rep. 69, 1 (1981).

[17] H. Sugawara and F. Von Hippel, Phys. Rev. 172, 176 (1968).

[18] H. Arenhövel, Nucl. Phys. A247, 473 (1975).

[19] H. Weber, Z. Phys. A 297, 261 (1980).

[20] H. Pilkuhn, *The Interaction of Hadrons* (Wiley, New York, 1967).

[21] M. Gourdin and Ph. Salin, Nuovo Cimento 27, 309 (1963).

[22] R. M. Woloshyn, E. J. Moniz, and R. Aaron, Phys. Rev. C 13, 286 (1976).

[23] R. Aaron, in *Modern Three-Hadron Physics,* edited by A. W. Thomas (Springer, New York, 1977), Chap. 5.

[24] R. Blankenbecler and R. Sugar, Phys. Rev. 142, 1051 (1966).

[25] A. Chodos and C. B. Thorn, Phys. Rev. D 12, 2733 (1975).

[26] J. R. Carter, D. V. Bugg, and A. A. Carter, Nucl. Phys. B58, 378 (1973).

[27] W. Pfeil and D. Schwela, Nucl. Phys. B45, 379 (1972).

[28] C. Betourne *et al.*, Phys. Rev. 172, 1343 (1968).

[29] R. L. Walker, Phys. Rev. 182, 1729 (1969) and references therein.

[30] G. Fisher *et al.*, Nucl. Phys. B16, 93 (1970).

[31] G. Fisher *et al.*, Nucl. Phys. B16, 119 (1970).

[32] K. H. Althoff *et al.*, Phys. Lett. 26B, 677 (1968).

[33] M. S. Bhatia and P. Narayanaswamy, Phys. Rev. 172, 1742 (1968).

[34] A. N. Kamal, Phys. Rev. 171, 1556 (1968).

[35] P. De Baenst, Nucl. Phys. B24, 633 (1970).

[36] A. Donnachie and G. Shaw, in *Electromagnetic Interactions of Hadrons,* edited by A. Donnachie and G. Shaw (Plenum, New York, 1978), pp. 143–157.